PERFORMANCE IDENTIFICATION OF THE APPARATUS FOR TESTING COMPACT HEAT EXCHANGER SURFACES

by

Branislav BAČLIĆ and Dušan GVOZDENAC

Original scientific paper
UDC: 536.24:66.045.1=20
BIBLID: 0354–9836, *1* (1997), 1, 73–92

The description of a new test apparatus designed for an on-line determination of flow friction and heat transfer characteristics of compact heat exchanger surfaces is given. The test section of the empty apparatus has been mathematically modelled for transient response. In order to increase the reliability of heat transfer data for compact heat exchanger surfaces obtainable on this apparatus, parameter identification of the empty test section model has been performed by an original statistical approach. The statistics in each run were based on 3 × 40 temperature data acquisition during the first 12 seconds after switching on the heater and the clock. One hundred experimental runs have been performed in order to identify the following parameters: (1) time constant of the exponential inlet temperature signal, (2) maximum fluid temperature rise at various mass flow rates for constant heater power supply, (3) number of fluid-to-wall heat transfer units, (4) time constants of two thermopiles to measure the temperatures up- and downstream of the matrix. Using humid air as the working fluid, each of these parameters is correlated at a high coefficient of determination with the Reynolds number in the range 10,770 < Re_a < 60,640.

Introduction

The transient techniques for evaluating average heat transfer coefficients for compact heat exchanger surfaces have been used for many years. There is a broad literature on the use of these methods, but the state in the field is certainly very challenging for new efforts to be made in order to eliminate some existent drawbacks, as well as to improve the overall reliability of the data reduction procedures. A need for improvement or replacement of most available transient test techniques used to establish the heat transfer design data for different matrix flow geometries has been stressed by London [5]. Shah [8] has also pointed to a need for transient tests with less than the existing experimental uncertainties of the Colburn factors. Typical reports that appeared after that time are those by Mullisen and Loehrke [7] and Cai *et al.* [3]. It is not our intention to review here the large number of preceding reports on the subject that have

led to the conclusions given by London [5] and Shah [8], but rather to present the guidelines that have been followed in designing a new transient technique in order to exclude some of the circumstances that might be the origin of the present unsatisfactory state in the field.

The goal was to develop a simple, inexpensive computer-controlled apparatus that will enable a fast determination of the basic heat transfer and flow friction data for a variety of compact heat exchanger surfaces, including the idea of simple sampling of the test cores. Manufacturing tolerances originating from various causes may significantly influence the performance of the heat exchanger surfaces. Geometrical imperfection of the flow passages as well as serial production imperfections like nonuniformity of brazing material distribution, etc., may show essential deviations from well-shaped and just-for-testing made cores. This may significantly effect the test results. The idea was to pick a random core sample straight from the production line and cut out the test piece by electro-erosion. This technique is also useful for investigating a core that in application cased to operate properly for various reasons (heavy fouling, corrosion, local damages due to bubble implosions in cryogenic two-phase applications of compact heat exchangers, *etc.*).

It is further descrable to have a transient test of short duration with rapid data reduction. Transient testing is closer to the real operational conditions since, in a majority of vehicular compact heat exchanger applications true steady conditions are rarely met. Short duration of a test justifies the use of a simple model since the effects of competing heat transfer mechanisms (axial conduction, radial conduction caused by heat losses and the like) cannot be detected in fluid temperature histories in the early stage of transients. Rapid data reduction impiles computer-controllable measurements as well as computer-based data processing. Recently such automated transient testing techniques are presented in the work of Mullisen and Loehrke [7] and Mochizuki and Yang [6]. It is also desirable that the underlaying method of both procedures, measurement and data reduction, has a deep physical meaning. This was accomplished by applying the *D*ifferential *F*luid *E*nthalpy *M*ethod (DFEM) (Bačlić *et al.* [1]) which is closely related to the overall heat balance of the test system.

Basic physical considerations indicate that the switching-on the electric heater, supplied by a constant power source, causes an exponential change of the fluid temperature. This realistic situation has to be accommodated by the model without any modification or misinterpretation at any stage of the data reduction method. Liang and Yang [4] advanced a single blow analysis based on an experimentally determined inlet fluid temperature response. By experiment, Liang and Yang [4] find the time constant of their heating screen and use this in their analysis to arrive at a theoretical exit air temperature response. By direct curve matching using five points, they determine the average heat transfer coefficient of the core. The purpose of the present work was to aim for an improved understanding of the exponential fluid temperature signal generated by the heater. Also, the role of the temperature sensor lag has to be recognized in rapid transient tests, but in a way that avoids unreliable prediction of the parameters determining this lag.

During the transient tests, heat is transferred from the fluid to the apparatus wall regardless of the fact that this flux is of a rather low intensity. A short test duration will ensure that the apparatus wall will not appreciably change due to finite fluid-to-wall

heat transfer. On the other hand, and due to the same reasons, the exponential fluid temperature disturbance generated by the heater will be skewed and attenuated by the time it reaches the matrix inlet.

All of these introductory remarks have formed a broad pathway that was followed in developing a new test apparatus for an on-line determination of heat transfer characteristics of compact heat exchanger surfaces.

This paper described the apparatus itself and the method of its parameter identification. The companion paper (Bačlić *et al.* [2]) contains the results of the experiments with a particular test matrix.

Description of the apparatus

In the description that follows, the underlined numbers in the parenthesis is designate particular devices from Fig. 1, which is a complete scheme of the apparatus. The apparatus is located in a completely air-conditioned laboratory so that the ambient air temperature and humidity are adjustable and controllable. The main part of the apparatus is an insulated PVC tube (1) through which the ambient air flow is induced by a variable speed axial fan (2). The fan speed is controlled by the voltage variator (3) so that a maximum apparatus Reynolds number (Re_d) of 62.000 is achievable. The mass flow rate through the apparatus tube was determined from standard (DIN 1952) orifice measurements. The orifice (4) static pressure drop was measured (with ±0.25 mm H_2O accuracy) by the micromanometer (5). A digital thermometer (6) was used to measure (with ±0.05 °C) the air temperature upstream of the orifice, while a differential manometer (7) measured (with ±0.5 mm H_2O) the static pressure in front of the orifice. Barometer (8) readings (with ±0.5 mbar), and electric psychrometer (9) wet and dry bulb temperature measurements (±0.1 °C) were used in combination with the above orifice measurement. The experimental compressibility factor and the Reynolds number correction of the orifice discharge coefficient are properly accounted for with the humid air properties included in the relevant orifice calculations.

The vertical part of the apparatus tube contains the test section as presented in Fig. 2. This section can be disassembled (not presented in the figures) into three parts: one joint is just under the test matrix (10) location, and the other just under the heater (11) location. The heater (11) is made of 0.18 mm kanthal filament with a resistivity of 53.1 Ω/m. It is threaded through the holes of an asbestos board ring to form a zigzag screen across the flow direction. When supplied with 250 V AC from the variable transformer (12), the heater power consumption was 610 W at any air flow rate within the region covered by the present experiments. Power was measured by a wattmer (13).

Two taps in the tube wall, at each location denoted by SP1 and SP2 in Fig. 3, were connected together to yield an average static pressure. Average static pressure drop between these taps was measured (with ±0.5 mm H_2O) by the differential micromanometer (14) and used for the estimation of an average friction factor for the heat transfer surface. No such pressure drop was detected in the empty test section.

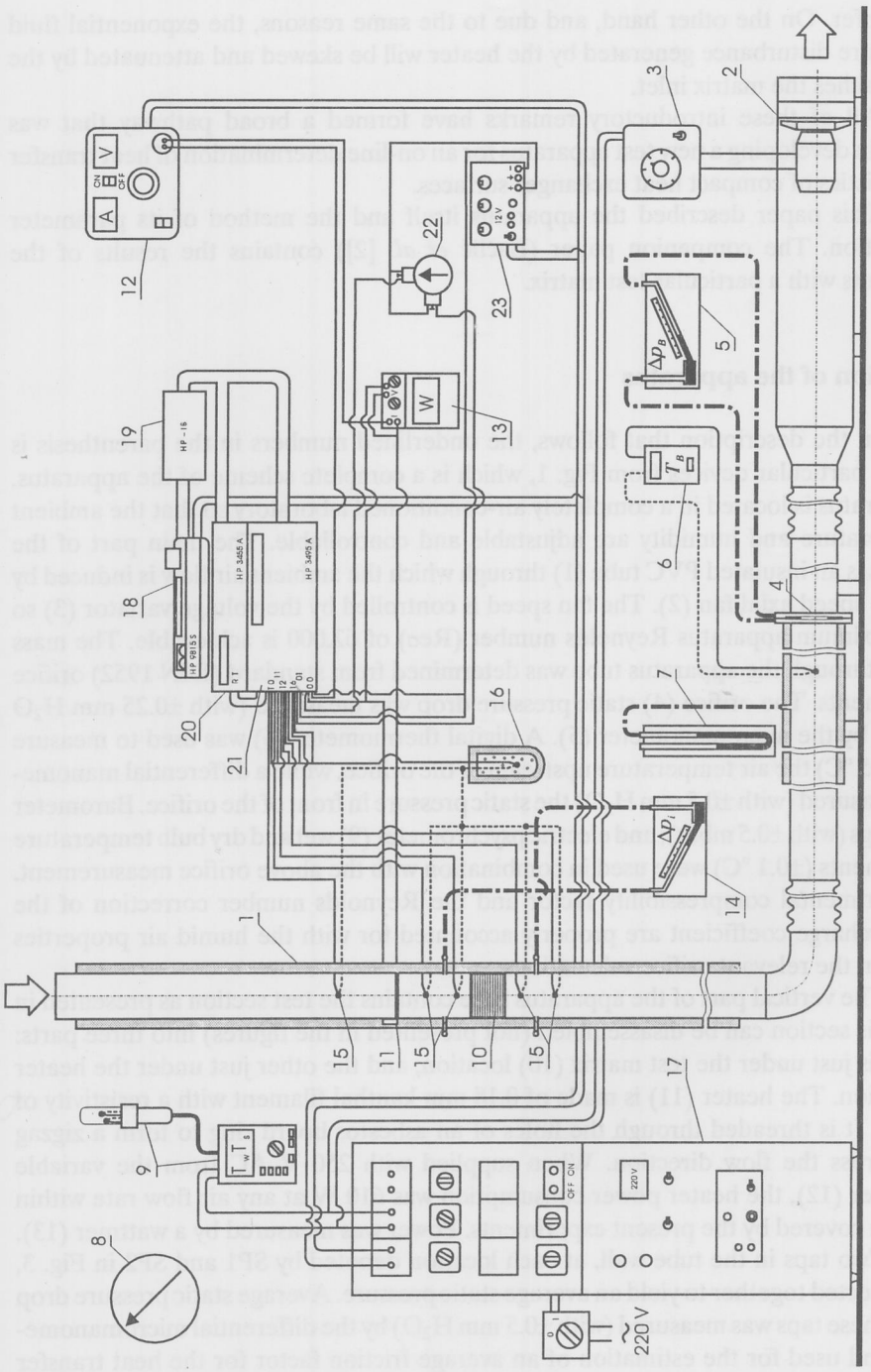

Figure 1. Apparatus outline (legend given in the text)

Air temperatures at various locations were measured by five thermopiles (15) (denoted by TP0 – TP4 in Fig. 2), each consisting of five 0.2 mm iron-constant thermocouples connected in series to yield an amplified emf. The cold point (16) (ice bath) is common. Thermocouple leads are conducted through two 3 mm plastic straws crossed along perpendicular diameters of the apparatus tube and sealed in the wall. Thermocouple junctions, facing upstreamwise at TP0 anddownstreamwise at the other locations, protrude 2 mm out of the straws. This simple design provided sufficient protection from the direct heather radition. Two temperature sensors (TP4 and TP1) are situated upstream of the matrix in order to enable accurate prediction of the air temperature history at the actual matrix inlet location (L_{m1}), where no measurements are made. Similarly, two thermopiles (TP3 and TP2) are downstream from the matrix. These are intended to be use for a backward extrapolation in order to have the actual exit air temperature history at L_{m2} location. However, these procedures are not the subject of the present report: just the utilization of TP0, TP1 and TP2 thermopiles, in an empty apparatus in order to identify the performance parameters, will be described.

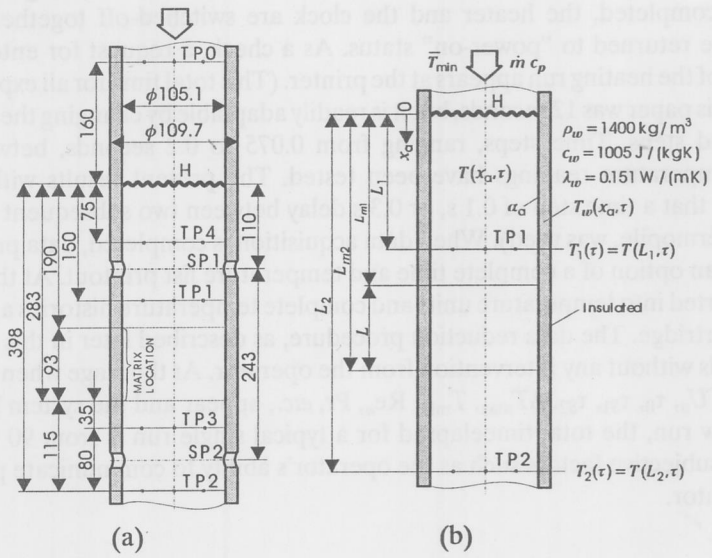

Figure 2. Apparatus tube test section: (a) basic measures: (b) notation used

The same three thermopiles are sufficient for matrix testing as described in [2].

All electrical and electronic devices are supplied from the (220 V, 50 Hz, 10 kVA) voltage servostabilizer (17). An HP 9815 S calculator (18) was used for all

communications and calculations. The calculator, through the HP-IB 98135A interface card (19), serves as the controller of the HP 3455A digital voltmeter (20) and the HP 3495A scanner (21). The electric chronometer (22), supplied through a 12 V DC stabilizer (23), was switched on and off simultaneusly with the heater. Switching-on the temperature measurement channels was also controlled by the computer/controller.

Next a typical communication procedure with the calculator is described. Pressing the RUN key causes a request for run number, date and fan speed information to be entered. This is immediately followed by subsequent requests for entering the data on wet and dry bulb and orifice temperatures, barometer pressure, orifice static pressure drop and the test section pressure drop. All these readings are in sight of the operator. Whenthe data is entered, the calculator responds by printing air humidity and mass flow rate data together with a warning that the apparatus is empty if zero test section pressure drop has been entered. Next is the warning to check that the heater power supply is set on. When the heater feed voltage is entered, the whole procedure for the next 12 seconds is completely under the programm control. The only information printed is that 40 cycle of subsequent TP0, TP1 and TP2 readings will be made. At that stage the voltmeter operation mode and the clock zero time are set first. Then the heater and the clockare switched-on together, and the sequence of 40 cycles of temperature readings is started. When this is completed, the heater and the clock are switched-off together and all instruments are returned to "power-on" status. As a check, a request for entering the total duration of the heating run appears at the printer. (This total time for all experiments presented in this paper was 12 seconds, but it is readily adaptable by changing the software clock command steps. Time steps, ranging from 0.075 to 0.2 seconds, between two subsequent temperature readings have been tested. The present results with 3 × 40 readings mean that a time step of 0.1 s, or 0.3 s delay between two subsequent readings of the same thermopile, was used). When data acquisition is completed, data processing is started with an option of a complete time and temperature list printout. At that stage, emfs are converted into temperature units and complete temperature histories are stored on an utility cartridge. The data reduction procedure, as described later in this paper, is done afterwards without any intervention from the operator. At the stage when the final results, like NTU_a, τ_0, τ_{S1}, τ_{S2}, ΔT_{max}, T_{min}, Re_a, Pr, *etc.*, appear and the system becomes ready for a new run, the total timeelapsed for a typical single run is from 90 to 120 s, depending on subjective factors such as the operator's ability to communicate promptly with the calculator.

Mathematical model of the test section

The purpose of the mathematical model of the apparatus test section (see Fig. 2b) is to provide means for reliable prediction of the fluid temperature history $T(L_{m1}, \tau)$ at the location ($x = L_{m1}$) where the test matrix entrance will be situated. It is assumed, on the basis of physical considerations, that the heater located at $x_a = 0$, when suddenly switched-on, generates the following change of the steady air flow temperature:

$$T(0,\tau) = \overline{T}_{\min} + \Delta T_{\max}\left[1 - e^{-\frac{\tau}{\tau_0}}\right] \tag{1}$$

where t_0 is the time constant of the apparatus, $\Delta T_{\max}$ is the maximum fluid temperature rise, and $\overline{T}_{\min}$ is the lowest temperature in the system. None of these parameters was intended to be subject of a prediction. They are identified experimentally.

To achieve the above goal, an idea of recording the temperatures $Y_1(\tau)$ and $Y_2(\tau)$ of the thermopile TP1 and TP2, located at $x_a = L_1$ and $x_a = L_2$, respectively, was in mind. These measurements have to replace the actual fluid temperature histories $T_1(\tau) \equiv T(L_1, \tau)$ and $T_2(\tau) \equiv T(L_2, \tau)$ at the same respective locations. To connect the relevant parameters of the system, the air-to-emoty test section transient heat transfer, as well as the temperature sensors dynamics have been modelled.

For transient heat transfer in the empty test section, the radially-lumped and axially-differential formulation of the problem, when axial-conduction effects neglected, results in

$$\frac{\partial \theta_w}{\partial u} + NTU_a(\theta_w - \theta) = 0 \tag{2}$$

$$C^* \frac{\partial \theta}{\partial u} + \frac{\partial \theta}{\partial \xi} + NTU_a(\theta - \theta_w) = 0 \tag{3}$$

for $0 \le \xi \le 1$, $u > 0$. Initially the system is at the minimal temperature

$$\theta_w(\xi,0) = \theta(\xi,0) = 0 \tag{4}$$

then the inlet fluid temperature is suddenly changed according to the relation

$$\theta(0,u) = 1 - e^{-\frac{u}{u_0}} \tag{5}$$

It is assumed that the apparatus number of the transfer units is small ($NTU_a < 1$), that is that the test section quickly responds to the temperature changes caused by sudden turning on the heater. These assumptions lead to the study of such a behavior of the system where $u_0 NTU_a \ll 1$. (In the experiments presented in this paper, this condition was fulfilled as: $0.032 < u_0 NTU_a \le 0.164$). It is well known (see, for example, Figs. 1a and 1b in [3], or Fig. 4 in [1] that under such a situation the dimensionless fluid temperature history is of a "quasi-exponential" type, with a very slow tendency to unity (almost with an asymptotic value less than one) for large dimensionless times. To obtain such a solution we introduce the "stretched" time variable $z = u/u_0 = \tau/\tau_0$ and rewrite the governing equations (2) and (5) in the form:

$$\frac{\partial \theta_w}{\partial z} + u_0 NTU_a(\theta_w - \theta) = 0 \tag{6}$$

$$\frac{\tau_d}{\tau_0}\frac{\partial \theta}{\partial z} + \frac{\partial \theta}{\partial \xi} + NTU_a(\theta - \theta_w) = 0 \tag{7}$$

$$\theta_w(\xi,0) = \theta(\xi,0) = 0 \tag{8}$$

$$\theta(0, z) = 1 - e^{-z} \tag{9}$$

The zero order perturbation solution (for $u_0 NTU_a \to 0$) of these equations is

$$\theta_w(\xi, z) = 0 \tag{10}$$

and

$$\theta(\xi,z) = \begin{cases} 0, & \text{for } z = \tau/\tau_0 < x_a/\overline{w}\tau_0 \quad (11) \\ e^{-NTU_a \xi}\left[1 - e^{-(z - x_a/\overline{w}\tau_0)}\right] & \text{for } z = \tau/\tau_0 \geq x_a/\overline{w}\tau_0 \quad (12) \end{cases}$$

Equation (10) states that, under these circumstances, the wall temperature does not yet start to change. Equation (12), in original variables, states that the fluid temperature rise anywhere in the test section behaves like:

$$\Delta T(x_a,\tau) \equiv T(x_a,\tau) - \overline{T}_{\min} = \Delta T_{\max} e^{-\frac{x_a NTU_a}{L_2}\left[1 - e^{-\frac{\tau - x_a/\overline{w}}{\tau_0}}\right]} \tag{13}$$

This means that at the locations of temperature sensors TP1 and TP2 in terms of local times

$$\tau_l = \tau - \frac{L_l}{\overline{w}}, \qquad l = 1, 2 \tag{14}$$

the temperature rises are

$$\Delta T_l(\tau_l) \equiv T_l(\tau_l) - \overline{T}_{\min} = \Delta T_{\max} e^{-\frac{L_l NTU_a}{L_2}\left[1 - e^{-\frac{\tau_l}{\tau_0}}\right]} \tag{15}$$

It is not difficult to verify that the following time averaging of the functions (15) is time invariant:

$$\frac{1}{\tau_l}\int_0^{\tau_l} \Delta T_l(y)dy + \frac{\tau_0}{\tau_l}\Delta T_l(\tau_l) = a_l \quad l = 1, 2 \tag{16}$$

Here the constants

$$a_l = \Delta T_{\max} e^{-\frac{L_l NTU_a}{L_2}} \qquad l = 1,\ 2 \tag{17}$$

represent the maximum temperature rise attenuation at $x_a = L_1$ and $x_a = L_2$ locations. (In a realistic situation $\Delta T_{\max}$ is achievable just at $x_a = 0$).

Time invariants a_1 and a_2, Eq. (17), are very useful, since one can combine them to obtain either the number of transfer units,

$$NTU_a = \frac{L_2}{L_2 - L_1} \ln \frac{a_1}{a_2} \tag{18}$$

or the maximum temperature rise in the system,

$$\Delta T_{\max} = a_2 \left(\frac{a_1}{a_2} \right)^{\frac{L_2}{L_2 - L_1}} \tag{19}$$

where L_1 and L_2 are the test section constants. Therefore, one must identify a_1 and a_2 from the measurements in order to obtain $NTUa$ and $\Delta T_{\max}$. However, the measurements do not provide the actual temperature histories $\Delta T_l(\tau_l)$, but rather temperature histories of the sensors, $\Delta Y_l(\tau_l) \equiv Y_l(\tau_l) - T_{\min}$ for $l = 1$ and 2. These can be related through the simplest model of the thermopile lag:

$$\tau_{Sl} \frac{d\Delta Y_l(\tau_l)}{dT_l} + \Delta Y_l(\tau_l) - \Delta T_l(\tau_l) = 0 \tag{20}$$

$$\Delta Y_l(0) = 0 \tag{21}$$

where $\tau_{Sl} = [(m_S c_S)/(A_S \alpha_S)]_l$, with $l = 1$ or 2, is the time constant of the respective temperature sensor. Since, as already mentioned, these sensors are of an in-series coupled-thermopile type, the prediction of parameters defining these time constants becomes questionable. For that reason, it would be best if they could be identified from the same measurements as the other test section parameters. On the other hand, it is also desirable not to lose the simple way of determining NTU_a and $\Delta T_{\max}$ from a_1 and a_2 as given above. Then, a natural question arises: What is the time operator acting on the temperature history $\Delta Y_l(\tau_l)$, being the solution of Eqs. (20) and (21) with $\Delta T_l(\tau_l)$, given by equation (15), that yields the same time invariant a_l es given by equation (17)?

It can be easily proved by basic calculus that the answer to this question is:

$$\frac{\tau_0 + \tau_{Sl}}{\tau_l} \Delta Y_l(\tau_l) + \frac{1}{\tau_l} \int_{\tau_l}^{\tau_l} \Delta Y_l(y)dy + \frac{\tau_0 \tau_{Sl}}{\tau_l} \frac{d\Delta Y_l(\tau_l)}{d\tau_l} = a_l \tag{22}$$

for $l = 1$ or 2. This is the key result to be used in the test section parameter identification. It interrelates, in a simple way, all the parameters (τ_0, τ_{Sl}, $\Delta T_{\max}$, NTU_a, L_1, L_2) with the

temperature histories $\Delta Y_l(\tau_l)$, $l = 1, 2$. A connoisseur will recognize that Eq. (22) is a kind of PID (*P*roportional-*I*ntegral-*D*ifferential) relation. It suggests that $\Delta Y_l(\tau_l)$ has to be experimentally recorded in a reliable way so that the operators on the LHS of Eq. (22) could be performed accurately by numerical procedures at any local time τ_l. The statistical method of experimental data processing is given in the next section. Note that once τ_0, NTU_a and ΔT_{max} are known for a particular run, the temperature $T(L_{m1}, \tau)$ at the test matrix inlet location is known as well. Also note that the existence of the time invariant for the problem under consideration enables the experimentalist to avoid the test of long duration that will cease to be adiabatic to the surroundings and/or generally to follow the basic assumptions. A remark, that fluid dwell times (x_a/w) are accounted in local times τ_l ($l = 1, 2$), is of interest as well. This fact is of importance with respect to the problems of fast scanning and of TP1 and TP2 thermopiles disposition at L_1 and L_2 locations, respectively. Finally, note that equation (16) has a deep physical meaning. When multiplied by the fluid capacity rate $\dot{m}c_p$ and local time τ_l, it governs the partition of the total fluid enthalpy change in the test section up to τ_l.

Experimental data processing

Discrete temperature measurements in a typical experimental run are presented in Fig. 3 by dots and crosses. Since thermopile TP0 located upstream of the heater

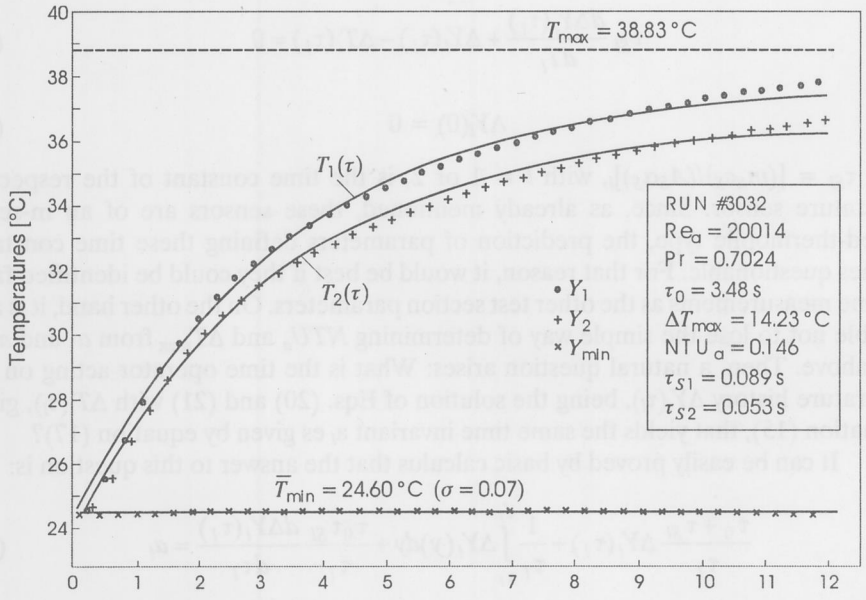

Figure 3. Empty test section temperature histories as measured (Y_1, Y_2 and Y_{min}) and resimulated (T_1 and T_2)

measures steady air temperatures $T_{\min,n}$ for $n = 1, 2, \ldots N$, $T_{\min}$ is simply the arithmetic mean of N readings ($N = 40$ is used in present experiments):

$$\overline{T}_{\min} = \frac{1}{N}\sum_{n=1}^{N} Y_{\min,n} \tag{23}$$

The σ in Fig. 3 indicates the standard deviation of this mean.

Next a derivation of the basic equations for statistical identification of the apparatus parameters from discrete $Y_{1,n}$ and $Y_{2,n}$ ($n = 1, 2, \ldots, N$) measurements is presented. Let

$$\beta_l = \tau_0 + \tau_{Sl} \tag{24}$$

and

$$\gamma_l = \tau_0 \tau_{Sl} \tag{25}$$

($l = 1, 2$) be the sums and the products of the time constants, respectively. Then at the exact solution at any discrete local time $\tau_{l,n}$ ($n = 1, 2, \ldots, N$) equation (22) must be valid:

$$\beta_l \hat{F}_{l,n} + \hat{I}_{l,n} + \gamma_l \hat{D}_{l,n} - a_l \tau_{l,n} = 0 \tag{26}$$

($l = 1, 2; n = 1, 2, \ldots, N$), where

$$\hat{F}_{l,n} = \Delta Y_l(\tau_{l,n})\big|_{exact} \tag{27}$$

$$\hat{I}_{l,n} = \int_0^{\tau_{l,n}} \Delta Y_l(y)dy\Big|_{exact} \tag{28}$$

$$\hat{D}_{l,n} = \left.\frac{d\Delta Y_l}{d\tau_l}\right|_{\substack{\tau_l=\tau_{l,n} \\ exact}} \tag{29}$$

However, experimental measurements and discrete data processing at the same specified discrete local times $\tau_{l,n}$ will yield the errors:

$$\Delta_{l,n} = \beta_l F_{l,n} + I_{l,n} + \gamma_l D_{l,n} - a_l \tau_{l,n} \tag{30}$$

($l = 1, 2; n = 1, 2, \ldots, N$), where

$$F_{l,n} = \Delta Y_{l,n} = Y_{l,n} - \overline{T}_{\min} \tag{31}$$

with $Y_{l,n}$ as measured and $\overline{T}_{\min}$ as computed from Eq. (23). The integrals $I_{l,n}$ appearing in Eq. (30) can be consecutively evaluated by the trapesoidal integration,

$$I_{l,n} = I_{l,n-1} + \frac{1}{2}\left(F_{l,n} + F_{l,n-1}\right)\left(\tau_{l,n} - \tau_{l,n-1}\right) \tag{32}$$

while the differential term $D_{l,n}$ can be substituted by central differences

$$D_{l,n} = \frac{F_{l,n+1} - F_{l,n-1}}{\tau_{l,n+1} - \tau_{l,n-1}} \tag{33}$$

for $n = 1, 2, ..., N-1$. Thus, $N-1$ errors of the form given by Eq. (30) can be found from a total number of N collected temperature readings of TP1 and as many from the readings of TP2.

Minimization of the sum of absolute values of the experimental errors leads to the least square conditions

$$\frac{\partial}{\partial \beta_l}\sum_{n=1}^{N-1}\Delta_{l,n}^2 = 0;\quad \frac{\partial}{\partial \gamma_l}\sum_{n=1}^{N-1}\Delta_{l,n}^2 = 0;\quad \frac{\partial}{\partial a_l}\sum_{n=1}^{N-1}\Delta_{l,n}^2 = 0 \tag{34}$$

($l = 1, 2$) as the criteria for determining β_l, γ_l and a_l for $l = 1, 2$. These conditions yield two sets of three linear algebraic equations of the form:

$$\begin{bmatrix} \sum_{n=1}^{N-1} F_{l,n}^2 & \sum_{n=1}^{N-1} F_{l,n}D_{l,n} & -\sum_{n=1}^{N-1} F_{l,n}\tau_{l,n} \\ \sum_{n=1}^{N-1} F_{l,n}D_{l,n} & \sum_{n=1}^{N-1} D_{l,n}^2 & -\sum_{n=1}^{N-1} D_{l,n}\tau_{l,n} \\ \sum_{n=1}^{N-1} F_{l,n}\tau_{l,n} & \sum_{n=1}^{N-1} D_{l,n}\tau_{l,n} & -\sum_{n=1}^{N-1} \tau_{l,n}^2 \end{bmatrix} \begin{bmatrix} \beta_l \\ \gamma_l \\ a_l \end{bmatrix} = \begin{bmatrix} \sum_{n=1}^{N-1} F_{l,n}I_{l,n} \\ \sum_{n=1}^{N-1} D_{l,n}I_{l,n} \\ \sum_{n=1}^{N-1} I_{l,n}\tau_{l,n} \end{bmatrix} \quad l = 1, 2 \tag{35}$$

Once β_l and η_l ($l = 1, 2$) are known from these equations, τ_{S1} and τ_{S2} can be eliminated by using Eqs. (24) and (25), to give the time constant τ_0, and afterwards τ_{S1} and τ_{S2} are readily obtainable from Eqs. (25), a_1 and a_2 as obtained from equations (35) can be then used in Eqs. (18) and (19) to yield NTU_a and ΔT_{max}, respecitively. Maximum temperature (see the T_{max} line in Fig. 3) is then simply predicted as $T_{max} = \Delta T_{max} + T_{min}$.

Having thus, in a particular run, all the parameters of the empty test section system, one can simulate actual fluid temperature histories at any location.

Curves $T_1(\tau)$ and $T_2(\tau)$ in Fig. 3 illustrate these at TP1 and TP2 location, respectively. Since $L_1 < L_{m1} < L_2$, the exponential temperature signal at the test matrix inlet location ($x_a = L_{m1}$), when calculated from Eq. (13) would lie between these two curves.

Closing this section a note should be made that the values of man humid air velocity were taken to be $\overline{w}_l = 4\dot{m}/(\pi D_i^2 \overline{\rho}_l)$ in local time calculations. Mass flow rate, $\dot{m}$, as obtained from the orifice readings (before turning on the heater) was used. However, the software was arranged so that the local humid air densities $\overline{\rho}_l$ ($l = 1, 2$) corresponding to the instantaneous (in real time τ) temperatures $Y_l(\tau)$, ($l = 1, 2$), have

corresponding to the instantaneous (in real time τ) temperatures $Y_l(\tau)$, ($l = 1, 2$), have been taken as the reference values. Since $T_{min} < Y_l(\tau)$, this was a suitable choice for taking into account the air flow acceleration at early stage of transients when the air temperature rises quickly. The final results of a single run experimental data processing, as described above, have been associated to the corrected values of Re_a and Pr numbers obtained by humid air physical properties evaluation at $T_{min} + \Delta_{max}/2$ as the reference temperature.

Results and discussion

To cover the variable fan speed range between 20% and 100%, one hundred experimental runs have been randomly selected in order to establish the apparatus Reynolds number dependence of all parameters. Each of these runs has been subjected to the data reduction procedure as described in the previous section, and each provided a set of results like those given in the box of Fig. 3. In such a way all the parameters have beendetermined in the range $10.770 < Re_a < 60.640$.

The results for the time constant of the exponential fluid temperature inlet signal versus Reynolds number are presented in the Fig. 4. A linear correlation of this log-log presentation resulted in

$$\tau_0 = 234.80\, Re_a^{-0.4266}\ [s] \tag{36}$$

with a coefficient of determination of 0.993. The reader should note the range of τ_0 values in Fig. 4.

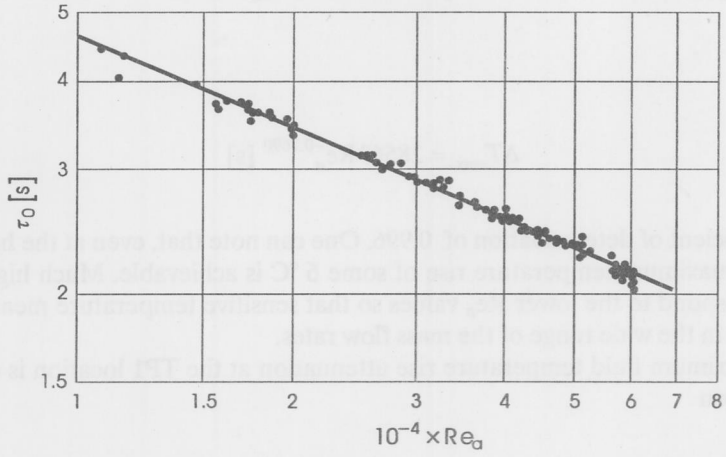

Figure 4. Time constant vs Reynolds number results

Maximum fluid-temperature-rise results at various mass flow rates for constant heater power supply are presented versus apparatus Reynolds number in Fig. 5. They are correlated by the equation

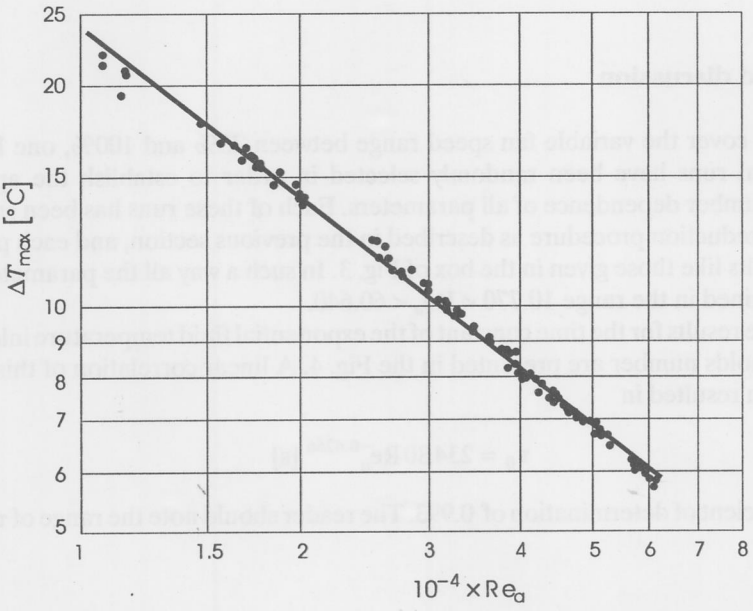

Figure 5. Maximum fluid temperature rise vs Reynolds number results

$$\Delta T_{max} = 28563 \, Re_a^{-0.7690} \; [s] \tag{37}$$

with a coefficient of determination of 0.996. One can note that, even at the highest Re_a values, the maximum temperature rise of some 6 °C is achievable. Much higher ΔT_{max} values correspond to the lower Re_a values so that sensitive temperature measurements are possible in the wide range of the mass flow rates.

Maximum fluid temperature rise attenuation at the TP1 location is correlated by the relation

$$a_1 = 21677 Re_a^{-0.7464} \; [°C] \tag{38}$$

with a coefficient of determination of 0.997. This correlation is presented in Fig. 6. Fig. 7 shows the corresponding results at the TP2 location. These are (with the same value of the coefficient of determination) correlated by the equation:

$$a_2 = 13738\,\mathrm{Re}_a^{-0.7094}\ [^\circ\mathrm{C}] \tag{39}$$

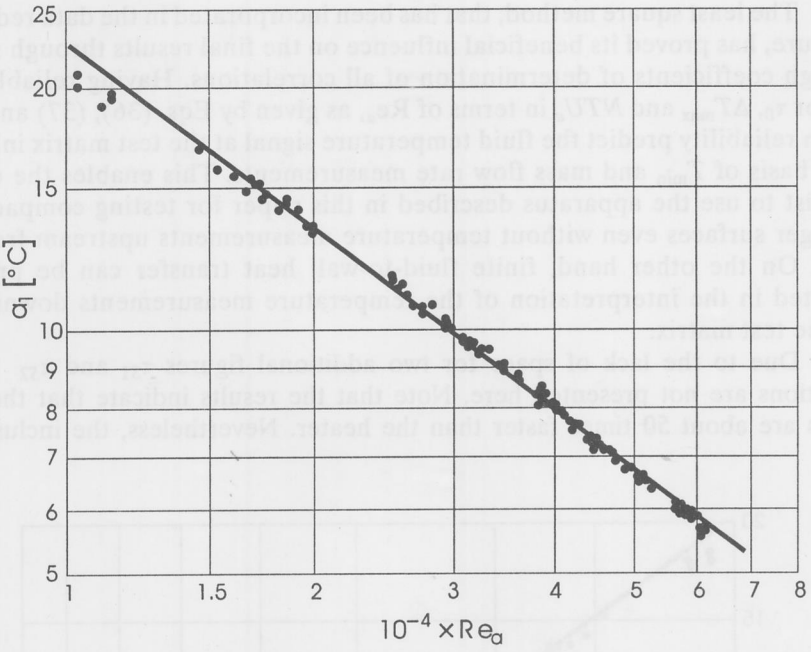

Figure 6. Maximum fluid temperature rise attenuation vs Reynolds number results at the TP1 location

When L_1 = 150 mm, L_2 = 398 mm and a_1 and a_2, from Eqs. (38) and (39), respectively, are substituted in Eq. (18), the following expression for the number of fluid-to-wall heat transfer units is obtained:

$$NTU_a = 0.7320 - 0.060 \ln \mathrm{Re}_a \tag{40}$$

For the Re_a range as given above, this equation gives $0.175 > NTU_a > 0.071$. It is worth noting that this semi-logarithmic correlation could be obtained from the basic data of each run as well. In such an approach the coefficients would be just

slightly different, but the coefficient of determination appears to be of the order of 0.6. This is because of the logarithmic amplification, see Eq. (18), of the particular deviations in a_1 and a_2 values. Since just time and temperature have been measured, it is natural that the results in corresponding units, that have been determined through a least square procedure, are correlated with higher coefficient of determination than the quantities that are indirectly calculated. These reasons lead to the decision that NTU_a vs Re_a relation should be obtained from already correlated a_1 and a_2 as above.

The least square method, that has been incorporated in the data reduction procedure, has proved its beneficial influence on the final results through noticeably high coefficients of determination of all correlations. Having reliable relations for τ_0, $\Delta T_{\max}$ and NTU_a in terms of Re_a, as given by Eqs. (36), (37) and (40), one can reliability predict the fluid temperature signal at the test matrix inlet just on the basis of $T_{\min}$ and mass flow rate measurements. This enables the experimentalist to use the apparatus described in this paper for testing compact heat exchanger surfaces even without temperature measurements upstream from the matrix. On the other hand, finite fluid-to-wall heat transfer can be properly accounted in the interpretation of the temperature measurements downstream from the test matrix.

Due to the lack of space for two additional figures τ_{S1} and τ_{S2} vs Re_a correlations are not presented here. Note that the results indicate that the thermopiles are about 50 times faster than the heater. Nevertheless, the inclusion of

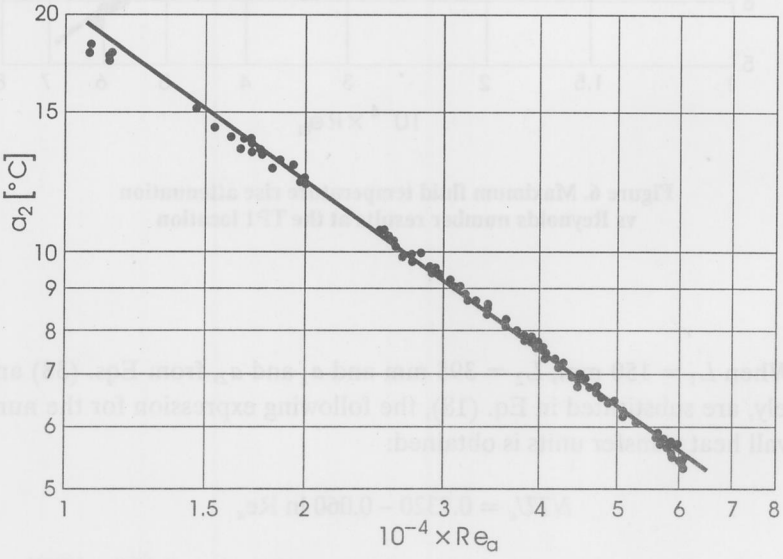

Figure 7. Maximum fluid temperature rise attenuation vs Reynolds number at the TP2 location

temperature sensors dynamic at the early stage of transients in the system, has proved to be decisive in obtaining the results presented.

Concluding remarks

The presented method of performance identification of the apparatus for testing compact heat exchanger surfaces is sufficiently general and simple to apply even to test sections designed differently than the one described here. The complete set of runs can be readily repeated in cas of any change in the apparatus performance (replacement of a new heater, corrosion of thermocouple junctions, *etc.*). Our experience shows that a single day is sufficient for a new set of runs in order to establish the apparatus performance. With no changes being made in the apparatus operation conditions, the results presented in this paper are absolutely reproductive. The final results of this work enable an accurate prediction of the fluid temperature signal at the matrix inlet as well as the proper accounting of the finite heat transfer to the apparatus wall. It is believed that the present approach is recommendable as a standard procedure to be performed prior to any transient single-blow test of compact heat exchanger surfaces.

Nomenclature

A_S [m^2]	– surface area
a_1 [°C]	– maximum temperature rise attenuation, defined by Eq. (17)
C_m^*	– fluid to wall thermal capacity ratio, dimensionless
c_p [J/(kg K)]	– specific heat at constant pressure
c_S [J/(kg K)]	– specific heat of the temperature sensor material
c_w [J/(kg K)]	– specific heat of the wall material
D [°C]	– designates local time derivative of the sensor temperature rise
D_i [m]	– inside diameter of the apparatus tube
D_o [m]	– outside diameter of the apparatus tube
$F = \Delta Y$ [°C]	– sensor temperature rise
H	– heater designation in Fig. 2
I [°C s]	– designates integration of the sensor temperature rise with respect to local time
L [m]	– test matrix length in Fig. 2
L_1 [m]	– heater to TP1 distance
L_2 [m]	– apparatus test section length, heater to TP2 distance
L_{m1} [m]	– heater to test matrix inlet location distance
L_{m2} [m]	– heater to test matrix exit location distance
$\dot{m}$ [kg/s]	– mass flow rate
m_f [kg]	– fluid mass occupying the test section
m_S [kg]	– mass of the temperature sensing elements
m_w [kg]	– mass of the test section wall
N	– total number of scanning cycles
NTU_a	– number of fluid-to-wall heat transfer units, dimensionless

Pr – Prandtl number, dimensionless
Re_a – apparatus Reynolds number, dimensionless
SP1, SP2 – designates static pressure taps in Fig. 2
T [°C] – temperature, fluid temperature
T_1 [°C] – fluid temperature at TP1 location
T_2 [°C] – fluid temperature at TP2 location
$\overline{T}_{min}$ [°C] – statistical mean minimum temperature in the system
$T_{min,n}$ [°C] – discrete value of minimum fluid temperature
TP0, TP1, TP2, TP3, TP4 – designate thermopiles in Fig. 2
u – dimensionless time variable
u_0 – dimensionless time constant of the exponential fluid temperature signal
$\overline{w}$ [m/s] – mean fluid velocity through the apparatus tube
x_a [m] – coordinate along the flow direction (see Fig. 2b)
Y_1 [°C] – temperature of TP1 sensor
Y_2 [°C] – temperature of TP2 sensor
$Y_{min,n}$ [°C] – discrete value of TP0 temperature
y [s] – dummy variable of the integration with respect to time
α_a [W/(m² K)] – fluid-to-wall heat transfer coefficient
α_S [W/(m² K)] – fluid-to-temperature sensor heat transfer coefficient
β [s] – sum of time constants, defined by Eq. (24)
γ [s²] – product of the time constants, defined by Eq. (25)
$\Delta_{l,n}$ [°C s] – discrete experimental error, defined by Eq. (30)
ΔT [°C] – fluid temperature rise
ΔT_l – local (l = 1, 2) fluid temperature rise
ΔT_{max} [°C] – maximum fluid temperature rise
ΔY_l [°C] – thermopile temperature rise
θ – dimensionless fluid temperature
θ_w – dimensionless wall temperature
λ [W/(m K)] – thermal conductivity of the fluid
λ_w [W/(m K)] – thermal conductivity of the wall material
μ [Pa s] – viscosity
$\xi = x_a/L_2$ – dimensionless coordinate
ρ [kg/m³] – fluid density
$\overline{\rho}_l$ [kg/m³] – reference value of the local fluid density
ρ_w [kg/m³] – density of the wall material
σ [°C] – standard deviation
τ [s] – time variable
τ_0 [s] – time constant of the exponential fluid temperature signal
τ_d [s] – dwell time, or transit time of fluid particle in the empty test section
τ_l [s] – local time variable
τ_{Sl} [s] – time constants of TP1 (l = 1) and TP2 (l = 2) thermopile

*

$$C_m^* = (m_f c_p)/(m_w c_w)$$

$$m_f = \rho D_i^2 \pi L_2 / 4$$

$$m_w = \rho_w (D_0^2 - D_i^2)\pi L_2 / 4$$

$$NTU_a = \alpha_a D_i \pi L_2 / (\dot{m} c_p)$$

$$\mathrm{Pr} = \mu c_p / \lambda$$

$$\mathrm{Re}_a = \rho \overline{w} D_i / \mu$$

$$u = \dot{m} c_p \tau / (m_w c_w)$$

$$u_0 = \dot{m} c_p \tau_0 / (m_w c_w)$$

$$\Delta T = T - \overline{T}_{\min}$$

$$\Delta T_{\max} = T_{\max} - \overline{T}_{\min}$$

$$\Delta Y_l = Y_l - \overline{T}_{\min}$$

$$\theta = (T - \overline{T}_{\min}) / \Delta T_{\max}$$

$$\theta_w = (T_w - \overline{T}_{\min}) / \Delta T_{\max}$$

$$\xi = x_a / L_2$$

$$\tau_d = L_2 / \overline{w}$$

$$\tau_{SI} = [m_S c_S / (A_S \alpha_S)]$$

Subscripts

1 – refers to TP1
2 – refers to TP2
n – an integer, scanning cycle counter
w – wall
l – thermopile location identifier, $l = 1$ for TP1, $l = 2$ for TP2

Superscripts

– exact value
– – mean or reference value

References

[1] Bačlić, B. S., Heggs, P. J., Abou Ziyan, H. Z. Z., Differential Fluid Enthalpy Method for Predicting Heat Transfer Coefficients in Packed Beds, Paper No. pp.–12, *8th International Heat Transfer Conference*, San Francisco, August 17–22, 1986

[2] Bačlić, B. S., Gvozdenac, D. D., Sekulić, D. P., Becić, E. J., Laminar Heat Transfer Characteristics of a Plate-Louver Fin Surface Obtained by the Differential Fluid Enthalpy Method, *Symposium on Advances in Heat Exchangers at 1986 ASME WAM*, (Eds., R. K., Shah and J. T., Pearson) Anaheim, CA, December 7–12, 1986

[3] Cai, Z. H., Li, M. L., Wu, Y. W., Ren, H. S., A Modified Selected Point Matching Technique for Testing Compact Heat Exchanger Surfaces, *Int. J. Heat Mass Transfer*, *27* (1984), pp. 971–989

[4] Liang, C. Y., Yang, W., Modified Single Blow Techniques for Performance Evaluation on Heat Transfer Surfaces, *ASME Journal of Heat Transfer, 97* (1975), pp. 16–21

[5] London, A. L., Compact Heat Exchangers – Unresolved Problems, *Fourth NATO Advanced Study Institute on Low Reynolds Number Forced Convection in Channels and Bundles – Applied to heat Exchangers*. Middle East Technical University, Ankara, Turkey, (1981), pp. 793–794

[6] Mochizuki, S., Yang, W. J., Performance Evaluation on Rotating Disk Assemblies by Automated Transient Testing Method, *Heat and Technology*, *4* (1986), pp. 1–21

[7] Mullisen, R. S., Loehrke, R. I., A Transient Heat Transfer Test for Computer-Based Data Reduction, *ASME* Paper 83-HT-65, 1983
[8] Shah, R. K., Research Needs in Low Reynolds Number Flow Heat Exchangers, *Heat Transfer Engineering*, *3* (1981), pp. 49–61

Authors addreess:

Prof. Dr. B. Bačlić, Prof. Dr. D. Gvozdenac,
Institute of Fluid, Thermal and Chemical Engineering
Mechanical Engineering Department, Faculty of Technical Sciences
University of Novi Sad
6, Trg Dositeja Obradovića
21121 Novi Sad, Yugoslavia